PHYSICAL REVIEW B VOLUME 19, NUMBER 4 15 FEBRUARY 1979

Electron states, one-electron density matrix and Fourier-transformed Compton profile of ordered and disordered one-dimensional potential arrays

P.Krusius
Electron Physics Laboratory, Helsinki University of Technology and Semiconductor Laboratory, Technical Research Center of Finland, SF-02150 Espoo 15, Finland

H. Isomäki
Department of General Sciences, Helsinki University of Technology, SF-02150 Espoo 15, Finland

B. Kramer*
Institüt fur Physik, Universität Dortmund, D-4600 Dortmund 50, Federal Republic of Germany
(Received 28 August 1978)

The properties of the one-electron density matrix of one-dimensional potential arrays have been studied using the transfer-matrix formalism. The potential arrays are constructed from square-well potentials with only the lowest even and odd states bound in order to facilitate an extension of the results to three-dimensional sp^n bonded systems. Infinite ordered arrays with filled bands (semiconductors, insulators) and with partially filled bands (metals), finite arrays and disordered arrays with structural, compositional and localized disorder are considered. It is shown that the one-electron density matrix, its spatial average (autocorrelation function or Fourier-transformed Compton profile), and the density of states converge rapidly with the cluster size irrespective of the boundary conditions or surface potentials used. The influence of disorder on the density matrix is investigated in detail for the discussion of real amorphous materials. It is concluded that localized disorder (point defects such as vacancies and iterstitials) has a more pronounced effect on the density matrix than extended disorder (structural or compositional). In addition, the relation between the autocorrelation function and the microstructure of the system is discussed and correlated with experimental findings. Finally, several new aspects for the interpretation of experimental autocorrelation functions are considered.

I. INTRODUCTION

Recently, it has been suggested to use Compton spectroscopy as a probe for the electronic states and the microstructure of molecules and solids.[1-5] In Compton spectroscopy one measures the differential cross section for inelastic x or γ rays. In the impulse approximation[6,7] this cross section is related to the ground-state momentum density $N(\vec{p})$ of the electron system. The one-dimensional Fourier transform of the Compton profile[5] (FCP) is given by

$$B(\vec{t}) = \int dr^3\, \Gamma_1(\vec{r}, \vec{r}+\vec{t}) = \int dp^3\, N(\vec{p}) e^{-i\vec{p}\cdot\vec{t}}, \qquad (1)$$

which shows the direct relation to the off-diagonal terms of the one-electron density matrix Γ_1. In the quantity $B(\vec{t})$, also called the autocorrelation function of the one-electron density matrix, core-state contributions are important only for very small values of t and may thus be separated from the valence-state contributions. Hence Compton scattering provides direct information on the properties of the valence-electron wave functions of molecules and solids.

Experimentally a large number of systems have been investigated ranging from the relatively simple atomic and molecular systems[1] to various metals, semiconductors, and insulators in ordered and disordered phases.[2,3,8-11] For atoms and small molecules the Compton profiles may be understood quantitatively in terms of the Hartree-Fock approach.[1,12] For large molecules and solids quantitative calculations, in the sense of, e.g., the local-density-dependent self-consistent formalism, are also possible but seem less satisfactory. The reasons for this are twofold: first, the application of these methods is extremely complicated, and second, the reproduction of the experimental results does not necessarily improve the physical understanding of the system because of the complicated computational procedures involved. The situation is somewhat similar as if one would attempt the interpretation of the optical spectra of idal crystals directly from the band structure without using selection rules, critical-point analysis, and van Hove singularities. It seems imperative to develop similar procedures for the analysis of wave-function-dependent quantities such as the Compton profile or the autocorrelation function. A first insight along these lines has already been found for periodic solids. For insulators or semiconductors it

follows from Bloch's theorem and full bands[5] that

$$B = (\vec{t} = \vec{R}_n \neq 0) = 0 \tag{2}$$

for lattice translations $\vec{R}_n$. Any further step requires basically complete knowledge of the one-electron density matrix. Therefore, one would like to know how the microstructure of a system in general influences the density matrix and, especially, what the role of order, structural or compositional disorder, and defects is. This would then, on the other hand, lead to an answer to the question on the nature of the information, which may be deduced from experimentally determined autocorrelation functions.

For periodic solids one may, of course, analyze the autocorrelation function by using the standard methods of band theory.[14-16] A more sophisticated analysis has been performed for the chalcogenide semiconductor selenium[13] based on the local-density-dependent self-consistent orthogonalized plane-wave approach. The results are in excellent agreement with experiment and show that for filled bands also other zeros of $B(t)$ may be interpreted as atom separations,[5] a property which by no means is trivial from the definition in Eq. (1). It has thus been shown that for ordered semiconductors or insulators the autocorrelation function contains information on the ground state to be read off directly.

For more complicated systems, such as disordered or large molecules, the situation is quite different. At present, one is not in a position to calculate autocorrelation functions with an accuracy comparable to that of the crystalline systems. Therefore, one has to resort to simple models and, in addition, to rather severe mathematical approximations. Two of the present authors have performed a first study along these lines using a generalized Koster-Slater impurity potential as the basic scattering potential.[17] In this work the amorphous phase was modeled by the random distribution of atomic scatterers and then compared with several crystalline phases. There is, however, an intrinsic problem associated with the Koster-Slater potential: the autocorrelation function of an isolated bound state of this potential is positive definite. As a result no direct extension of the results to, e.g., sp^n bonded systems is possible.

In this paper we present an analysis of atomic scatterers with nonpositive definite autocorrelation functions. However, in order to be able to study various kinds of disorder, defects, interstitials, and vacancies, the dimension of the system must be limited to one. This is not a serious restriction, since the autocorrelation function is continuous and does not contain any dimension-dependent singularities, as may be demonstrated easily, e.g., by considering the free-electron gas in one to three dimensions. We want to stress in this context that although a number of studies on the energy spectra and density of states for a variety of one-dimensional systems have been performed,[18] wave-function-dependent properties have rarely been studied.

The plan of the present paper is as follows. In Sec. II the one-dimensional model system is presented. Section III contains a brief description of the mathematical methods used and the accuracy achieved. In Sec. IV the results for ordered and disordered systems are given. The paper ends with a conclusion including the extensions of the results of the model study to real three-dimensional systems.

II. MODEL

When looking for suitable scattering potentials we must have in mind that for sp^n bonded systems the contributions of s- and p-type states to the autocorrelation function are positive and nonpositive definite, respectively. A simple one-dimentional potential, for which the bound states fulfill this requirement, is the square well. Hence we take it as the atomic scattering potential in our model. The total potential energy is written

$$V(x) = \sum_i U_i(x - x_i) . \tag{3}$$

The sytems is then characterized by the set of coordinates $\{x_i\}$ and the corresponding square wells $\{U_i\}$. Each well is completely defined by its width a_i and depth V_i. However, in order to have at least one odd bound state for the isolated well, the relation $V_i a_i^2 > \frac{1}{2}\pi^2$ must be fulfilled. As boundary conditions we assume either periodic boundary conditions or free decay conditions at the ends of the chain. In addition, for free states a surface potential V_s at a distance x_s large com-

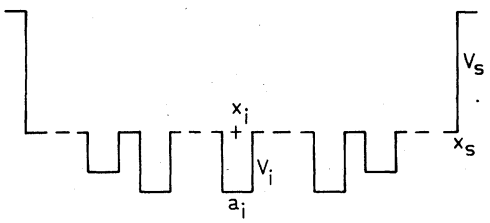

FIG. 1. Square-well potential array defined by the set of well parameters $\{x_i, a_i, V_i\}$ and the surface parameters $\{x_s, V_s\}$.

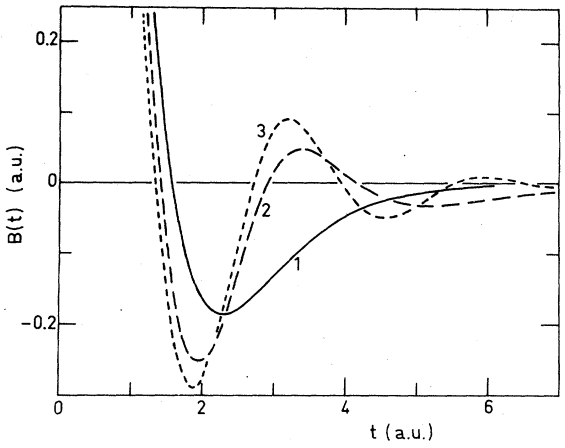

FIG. 2. Spatially averaged one-electron density matrix (autocorrelation function) $B_1(t)$, $B_2(t)$, and $B_3(t)$ for a system of one, two, or three wells (curves 1, 2, and 3, respectively) in atomic units. For each well $a = 2$ a.u. and $V = 3.6$ a.u. The nearest-neighbor separation measured from the well walls is $b = 0.5$ a.u. The norm is in all cases $B(0) = 2$ a.u.

pared to the dimensions of the system is introduced (Fig. 1). Of course, the actual choice of the boundary conditions does not affect the bulk properties of our model in the thermodynamic limit when the size of the system becomes sufficiently large.

As well for simplicity as to facilitate an extrapolation to sp^n bonded systems, we restrict the parameters of the isolated square well such that only the lowest even and odd states are bound. As our standard well we take $a = 2$ a.u., and $V = 3.6$ a.u. The associated autocorrelation function $B_1(t)$, normalized such that $B_1(0) = 2$, is shown in Fig. 2. $B_1(t)$ becomes negative at distances larger than $t_0 \approx 1.6$ a.u., which is comparable with the well width a, because the localization length of the odd state is greater than that of the even state.

III. METHOD

The one-particle Schrödinger equation associated with a piecewise constant one-dimensional potential is usually solved by applying the transfer matrix formalism.[18] Consider a discontinuity joining two intervals of constant potential i and $i+1$ on the left- and right-hand side of the discontinuity, respectively. Then the continuity conditions for both the wave function and its derivative may be written

$$T_i X_i = T_{i+1} X_{i+1} . \tag{4}$$

Here the 2×2 transfer matrices T and 2×1 solution vectors X depend on the energy of the state. Working through all discontinuities and applying the chosen boundary conditions at each end, one obtains a linear homogeneous system of equations for the amplitudes, i.e., the components of the vectors X. For example, for a periodic system the associated matrix $A(E)$ is cyclic with 2×2 blocks on the main diagonal, the lower subdiagonal, and in the upper right-hand corner. The dimension of the determinant of $A(E)$, which fixes the energies E_i, is then two times the number of discontinuities in the unit cell. Since, however, the inverses of the transfer matrices T exist, the determinant of $A(E)$ reduces to a 2×2 nonlinear determinant for the energies. Having solved the reduced determinant for the eigenvalues, one generates the solution vectors from the chain of equations (4). Since ground-state properties are strived at, care must be exercised in the case of degeneracies in order to find all state vectors.

As the procedure outlined above contains no mathematical approximation, the results are exact. Using only relative coordinates in the products of transfer matrices and double precision arithmetic with 18 significant decimal digits, high accuracy is achievable in practice too. The zeros of the reduced determinant were found by using Mueller's rapidly convergent iteration scheme of successive bisection and parabolic interpolation.[19] The autocorrelation function is calculated from the set of occupied eigenstates ψ_i according to

$$B(t) = \sum_i \int dx\, \psi_i(x)^* \psi_i(x+t) \tag{5}$$

by performing the integral over x analytically. For infinite periodic systems the resulting integral over the wave vector k is evaluated using the six-point Gauss-Legendre quadrature[20] for each interval of k. With a 36-point sampling the relative convergence for $B(t)$ associated with this k integration is typically less than 10^{-6} even for distances as large as three times the width of the individual scatterer a_i. The overall numerical accuracy is best described by the following: using for a periodic system with three wells per unit cell a relative energy threshold of 10^{-16} and a 36-point k sampling, the relative error $B(R_1)/B(0)$ for the autocorrelation function at the first Bloch zero R_1 [Eq. (2)] is of the order of 10^{-17}.

IV. RESULTS AND DISCUSSION

A. Molecular systems

The effect of interatomic interactions on the autocorrelation function can best be demonstrated by comparing the results $B_1(t)$, $B_2(t)$, and $B_3(t)$ for

one-, two-, and three-square-well systems, respectively (Fig. 2). Basically, the interaction between the bound states introduced a contraction of the wave functions and—even more important—additional oscillations into the autocorrelation function. In Fig. 2 the interwell separation has been chosen such that all the original bound states of the isolated wells remain bound. A major reduction of these separations would lead to a case with some of the uppermost states bounded only by the surface potential defined in Fig. 1. As $B_1(t)$, also $B_2(t)$ and $B_3(t)$ are negative definite for values of t larger than the size of the system.

In the present case the number of zeros n of $B(t)$ is in a simple manner related to the number of wells per molecule N via

$$n = 2Nn_1 - 1 , \tag{6}$$

where n_1 is the number of zeros of the single well autocorrelation function $B_1(t)$.

B. Infinite-ordered systems

The autocorrelation functions $B^1_\infty(t)$ and $B^3_\infty(t)$ for infinite systems with one or three wells per unit cell, respectively, are shown in Fig. 3. The nearest-neighbor separations are the same as those for the molecular systems in Fig. 2, and consequently all bound states of the corresponding isolated wells remain bound. The associated energy bands are plotted in Fig. 4 in order to give the reader more familiar description of the strength of the interactions. Three or one Bloch zero, of $B^1_\infty(t)$ or $B^3_\infty(t)$, respectively, are shown in Fig. 3. The number of zeros of $B_\infty(t)$ between two successive Bloch zeros [Eq. (2)] is also given by Eq. (6), if N is taken to be the number of wells per unit cell. $B^1_\infty(t)$ and $B^3_\infty(t)$ are for $t \lesssim 4$ a.u., qualitatively very similar with each other and even to a lesser degree also with $B_2(t)$ and $B_3(t)$. One realizes that the differences in the autocorrelation function between these four structures with an identical nearest-neighbor configuration increase with t and that the oscillations are completely out of phase for distances, which exceed the size of the identical structural unit. Further, it should be noted that all zeros of $B(t)$ seem to appear at multiples of basic intervals irrespective of whether they should exactly fulfill Eq. (2) or not.

For the present infinite ordered systems with completely filled bands the following set of equations for the zeros can be derived empirically:

$$t_1 = \tfrac{1}{2}\sum_i n_i b_i \Big/ \sum_i n_i . \tag{7}$$

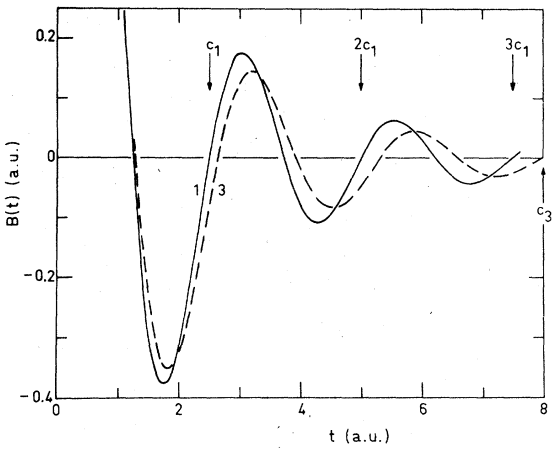

FIG. 3. Autocorrelation function $B^1_\infty(t)$ and $B^3_\infty(t)$ of infinite ordered arrays with one or three wells per unit cell (curves 1 and 3, respectively) and filled bands in atomic units. For each well $a = 2$ a.u. and $V = 3.6$ a.u. The nearest-neighbor separation is $b = 0.5$ a.u. and the next-nearest-neighbor separation for curve 3, $d = 1.0$ a.u. Both separations are measured from the well walls. The lattice translation is $c_1 = 2.5$ a.u. or $c_3 = 8.0$ a.u. for curves 1 and 3, respectively. The norm is in all cases $B(0) = 2$ a.u.

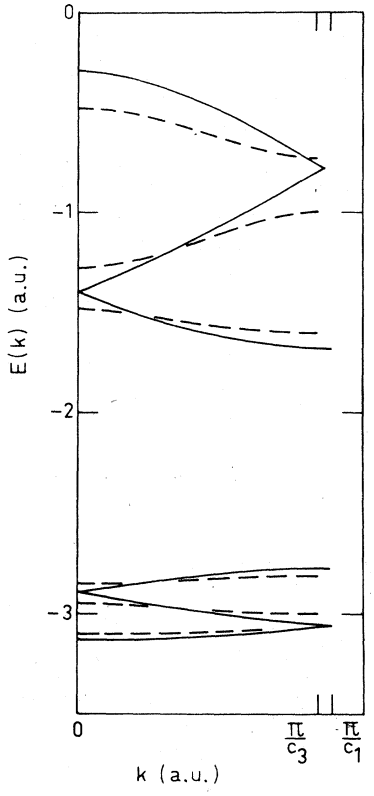

FIG. 4. Energy-band structure $E(k)$ for the periodic arrays of Fig. 3 with one (full curve) or three (dashed curve) wells per unit cell in atomic units. For other parameters see caption of Fig. 3.

$$t_2 = \sum_i n_i b_i \Big/ \sum_i n_i , \tag{8}$$

$$t_m = m_1 t_1 + m_2 t_2 . \tag{9}$$

t_i denotes the ordered sequence of zeros of $B(t)$, b_i is the neighbor separation in the system, n_i is the associated number of neighbor separations of type b_i, and m_1 and m_2 denote appropriate integral numbers. Equation (7) is the most approximate of the above equations.

The translation relation of Eq. (2) is no longer valid for periodic structures with incompletely filled bands. There are essentially two ways of introducing partly filled bands into the infinite arrays considered. The first is simply to vary the occupation (rigid-band metal) and the second is to increase the interactions between the bound states until part of them are pushed into the continuum (interaction metal). The results for both metallic systems based on a unit cell with three wells are displayed in Fig. 5. In both cases about one third of the states in the uppermost band are unoccupied. Comparing Figs. 3 and 5, one realizes that the effect of the partial occupation is small for correlation lengths below the dimensions of a single well, but that for larger values of t both the amplitudes and phases are essentially influenced. In addition, it is evident that the correlations in the metallic systems on the average are larger than for completely filled cases. For the one-dimensional free-electron gas the autocorrelation function is

$$B_{fe}(t) = B(0) \sin(p_F t)/p_F t , \tag{10}$$

where the Fermi momentum p_F only depends on the density of electrons. The zeros of $B(t)$ for the interaction metal, contrary to those of the rigid-band metal, are equidistant as for the free-electron gas. However, only by using an effective Fermi momentum, corresponding to a 10% higher density, in combination with Eq. (10) a fit for the zeros may be obtained, but even then the amplitudes deviate markedly. Therefore, it is evident that the interatomic interactions reduce the electron-electron correlations.

C. Finite-ordered systems

Consider now finite ordered arrays of the square-well scatterers. The key issue is to find out to what extent infinite systems may be modeled with finite clusters, if density-matrix-dependent quantities, such as the autocorrelation function, are of interest. There also remains the question of the choice of the boundary conditions and surface potentials. Examples of autocorrelation functions of finite ordered systems are given in Figs. 6 and 7 for 21-well arrays corresponding to the infinite periodic systems of Fig. 3. In Figs. 6 and 7 the free decay and the periodic boundary conditions, respectively, have been used. A more exact comparison of the key quantities associated with these finite and infinite sys-

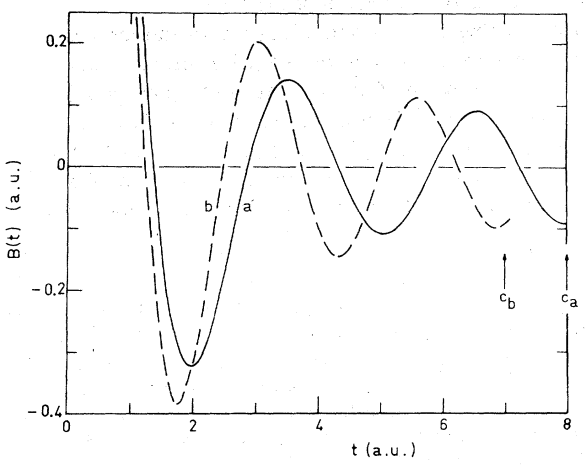

FIG. 5. Autocorrelation function of infinite ordered arrays with three wells per unit cell and partially filled bands in atomic units. (a) Rigid-band metal: parameters $a = 2$ a.u., $V = 3.6$ a.u., $b = 0.5$ a.u., $d = 1.0$ a.u., and $c_a = 8$ a.u., as in Fig. 3, but Fermi momentum at $k_F = \frac{1}{3}(\pi/c_a)$, i.e., uppermost band filled up to $\frac{2}{3}$ of total band. Norm is $B(0) = \frac{1}{3}(17/3)$ a.u. (b) Interaction metal: parameters $a = 2$ a.u., $V = 3.6$ a.u., $b = 0.25$ a.u., $d = 0.25$ a.u., and $c_b = 7$ a.u. k_F is at $\frac{1}{3}(\pi/c_b)$ and norm $B(0) = \frac{1}{3}(17/3)$ a.u.

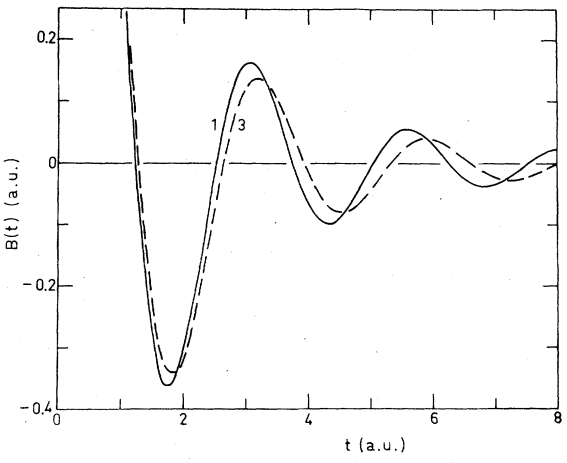

FIG. 6. Autocorrelation function for finite ordered arrays of 21 wells with one (curve 1) or three (curve 3) wells per unit cell. Free decay boundary conditions have been used and the parameters of the unit cells are the same as those in Fig. 3. Norm $B(0) = 2$ a.u.

TABLE I. Convergence of autocorrelation function $B(t)$ as a function of t and the cluster size. The unit cell contains one well with the parameters $a = 2$ a.u. and $V = 3.6$ a.u. The nearest-neighbor separation is $b = 0.5$ a.u. The column labels (N, FD) or (N, PB) define the number of unit cells N and the boundary conditions FD (free decay) and PB (periodic boundary).

	$B(t)$ (a.u.)					
t(a.u.)	(5, FD)	(12, FD)	(21, FD)	(38, FD)	(21, PB)	(∞, PB)
1.8	−0.3213	−0.3532	−0.3629	−0.3687	−0.3756	−0.3759
2.5	−0.0547	−0.0229	−0.0131	−0.0072	0.0000	0.0000
3.0	0.1159	0.1515	0.1624	0.1688	0.1768	0.1768
5.0	−0.0231	−0.0098	−0.0056	−0.0031	0.0000	0.0000
7.5	−0.0109	−0.0048	−0.0028	−0.0015	0.0000	0.0000

tems as well data on the convergence as a function of the size of the finite cluster is given in Table I. Comparing Figs. 7 and 3, one realizes that the 21-well cluster gives an almost complete quantitative convergence with respect to the infinite counterpart, if appropriate periodic boundary conditions are used for the cluster. The information from Fig. 6 is that the influence of the boundary conditions on the finite cluster remains small for correlation lengths t much smaller than the cluster size, just as one expects. The difference in the autocorrelation function induced by the boundary conditions for equal t is, however, somewhat larger than the convergence error resulting from the cluster size.

A similar good convergence, as for the autocorrelation function, can also be observed in the behavior of the density matrix itself (Table II)

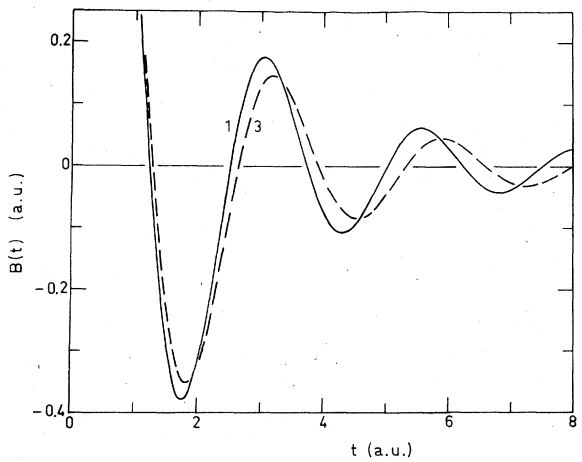

FIG. 7. Autocorrelation function for finite ordered arrays of 21 wells with one (curve 1) or three (curve 3) wells per unit cell. Periodic boundary conditions have been used and the parameters are the same as those in Fig. 6. Norm $B(0) = 2$ a.u.

and the density of states. For the latter the effects of the infinite resolution width has to be taken into account for all systems in a similar manner (Fig. 8). For example, the 21-well ordered array with three wells per unit cell the variance of the density of states with respect to the crystalline counterpart is 0.5%.[21] The extremely good convergence properties of the energy spectrum can even better be demonstrated by considering the separation ΔE between two eigenvalues associated with the finite system, which correspond to $E(k)$ and $E(-k)$ in the infinite case and which therefore tend to degenerate in the infinite limit. For bands associated with the bound states and periodic boundary conditions, one has maximally $\Delta E \approx 0.005\, E_B$, where E_B denotes the width of the corresponding band.

Interesting effects associated with the averaging property of the autocorrelation integral are found for compound arrays (alloys). The results for two ordered alloys, which differ either in well depth or well width, are presented in Fig. 9. In both cases the unit cell comprises two wells with different characteristics but with equal near-

TABLE II. Convergence of one-electron density matrix $\Gamma_1(x, x+t)$ as a function of t and the cluster size. The unit cell contains one well with the parameters $a = 2$ a.u. and $V = 3.6$ a.u. The nearest-neighbor separation is $b = 0.5$ a.u. The origin of the coordinate system x is at the inversion center of the arrays. The other columns are labeled as in Table I .

	Γ_1 (a.u.)			
$x, x+t$ (a.u.)	(1, FD)	(9, FD)	(15, FD)	(21, FD)
0, 0	0.708 602	0.765 868	0.766 095	0.766 101
0, 0.2	0.690 444	0.740 891	0.741 086	0.741 091
0, 1.0	0.299 554	0.251 337	0.251 129	0.251 124
0, 3.0	•••	0.067 702	0.067 973	0.067 980
0, 10.0	•••	−0.005 497	−0.004 147	−0.004 113

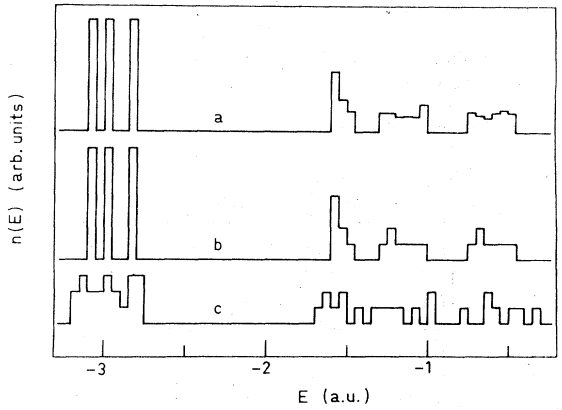

FIG. 8. Density of states $n(E)$ in atomic units for a resolution width of 0.05 a.u. In all cases the structure is based on the same unit cell with three wells and with the parameters used in Fig. 3: $a=2$ a.u., $V=3.6$ a.u., $b=0.5$ a.u., $d=1.0$ a.u., and $c=8$ a.u., (a) infinite ordered array of unit cells with periodic boundary conditions, (b) finite ordered array with a total of 21 wells and periodic boundary conditions, and (c) structurally disordered array with a random modulation of 50% of the parameters b and d and free-decay boundary conditions.

est-neighbor and next-nearest-neighbor separations measured from the well walls. A comparison with the corresponding elemental systems in Fig. 6 shows that the autocorrelation integral,

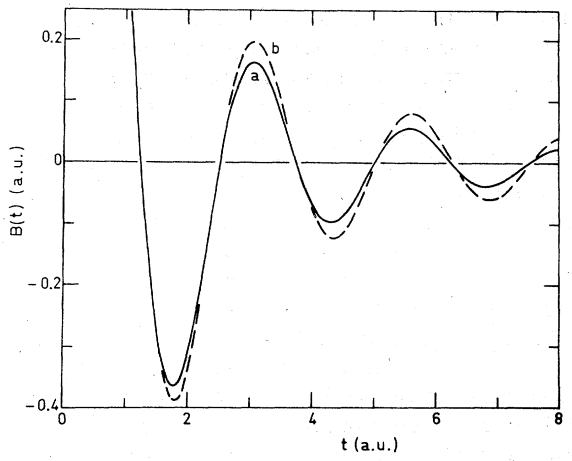

FIG. 9. Autocorrelation function of finite ordered two-component alloys with free-decay boundary conditions and two wells per unit cell. Length of chain is 11 unit cells; (a) parameters $a_1=2$ a.u., $a_2=2$ a.u., $V_1=3.8$ a.u., $V_2=3.4$ a.u. Separation of wells is $b=0.5$ a.u. from well walls and separation from unit cell boundaries $u=0.25$ a.u measured from the well walls; (b) parameters $a_1=1.65$ a.u. $a_2=2.35$ a.u., $V_1=3.6$ a.u., $V_2=3.6$ a.u. Separations defined as for case (a): $b=0.5$ a.u and $u=0.25$ a.u. Lattice translation $c=5$ a.u. and norm $B(0)=2$ a.u. in both cases.

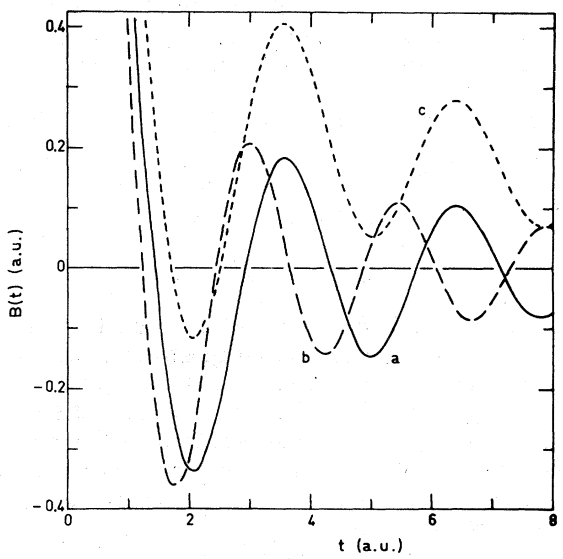

FIG. 10. Autocorrelation function for finite ordered arrays with partially filled bands. In all cases there is one well per unit cell and a total of 21 wells in the array. Free-decay boundary conditions have been used for bound states. (a) Rigid-band metal: parameters $a=2$ a.u., $V=3.6$ a.u., $b=0.5$ a.u. and Fermi level such that five states of all 42 are unoccupied. Norm is $B(0)=37/21$. (b) Interaction metal: parameters $a=2$ a.u., $V=3.6$ a.u., $b=0.115$ a.u. and states 1–37 of 42 bound. Norm is $B(0)=37/21$ a.u. (c) Metal with free states: parameters $a=2$ a.u., $V=2.9$ a.u., $b=0.5$ a.u., surface potential $V_s=10$ a.u., and surface positions $x_s=50$ a.u. symmetrically from center of system for the free states. States 1–37 are bound and five additional ones free. Norm is $B(0)=2$ a.u.

indeed, averages over the unit cell of the alloy in a straightforward geometrical sense defined by the corresponding unit cell potentials. The zeros of $B(t)$ for compound systems are also given by Eqs. (7)–(9).

Partial occupation of the isolated well derived states for the finite ordered systems has qualitatively a similar effect on the autocorrelation function as for infinite ordered arrays. In Fig. 10 the results for two finite metallic systems corresponding to the infinite insulating arrays of Fig. 6 are given. Figure 10 also shows a true metallic system with the number of the occupied states equal to the number of the original states of the isolated scatterers. For the free states the surface potential introduces the boundary conditions. It is interesting to note that the autocorrelation function for the latter states is of the slowly varying type, which for small values of t can be considered as an additive positive constant. This effect can easily be understood by considering the autocorrelation function of the

first few states of a particle in a box bounded by an infinite surface potential (see Fig. 1). One obtains for the even and odd states, respectively,

$$B_n^e(t) = \cos[(n-\tfrac{1}{2})\pi t/|x_s - x'_s|], \quad (11)$$

$$B_n^o(t) = \cos(n\pi t/|x_s - x'_s|), \quad (12)$$

both of which are constants for $t/|x_s - x'_s| \ll 1$.

D. Finite disordered systems

Finite disordered systems with any kind of disorder, whether structural, compositional, or induced by defects, vacancies, or interstitials, may be studied using the model potentials of Eq. (3). The comparison of the results for these systems with the corresponding properties of ordered counterparts facilitates conclusions on the influence of the various types of disorder on the one-electron density matrix of real three-dimensional materials. The restriction to finite clusters has no effect on these conclusions, since the cluster convergence was found to be almost complete.

Consider first pure structural or compositional disorder simulated by a random modulation of either the neighbor separations or the well depths. Results for arrays based on one type of well are given in Tables III and IV. Similar results may also be obtained for compound systems even with partially filled bands. The modulation percentages for the uniform symmetrical distribution have been chosen such that no excessive formation of localized states occurs, since the applied transfer-matrix approach begins to break down for a predefined accuracy of the floating point arithmetics if a certain level of localization is exceeded. Surprisingly enough, even a large amount of a structural or compositional disorder, which has profound effects on the density of states (Fig. 8), has a vanishingly small influence on the autocorrelation function. A more detailed analysis shows that although each state changes even by orders of magnitude, the net effect on $B(t)$ cancels approximately both between states of a band group and between band groups. In addition, configuration averaging even more reinforces the cancellation effect. This behavior can be understood, if one assumes that the occupied eigenstates of the disordered systems may obtained via an unitary transformation from the corresponding eigenstates of the ordered system. There is, however, no obvious justification for an assumption like this. As to the present case, the disorder is introduced in such a manner that no mixing between the occupied and virtual states occurs. Consequently, one can justify the above assumption with the aid of perturbation theory.

From the above discussion, it also follows that vacancies and interstitials should have a more pronounced effect on the autocorrelation function. This is precisely what happens, as may be seen from Fig. 11, where the results for two concentrations, 5% and 10%, of vacancies or interstitials are given. Two interesting features may be learned from these results. First, as expected, the effect of localized disorder on $B(t)$ scales roughly with concentration, and second, the influence is maximum at correlation lengths t, where the autocorrelation function of the ordered counterpart becomes zero. The latter behavior follows from the fact that the zeros of $B(t)$ are

TABLE III. Influence of structural disorder on the autocorrelation function $B(t)$. As reference the finite ordered array of 21 wells with a unit cell of one well is used. The parameters are $a = 2$ a.u., $V = 3.6$ a.u., and $b = 0.5$ a.u. The columns denoted by $\Delta B^1_{N;M}$ give the difference of the autocorrelation function of the structurally disordered array with $M\%$ modulation of b and the ordered array in units 10^{-4} a.u. In the two right-most columns the contributions of the lower (states 1–21) and upper (states 22–42) band groups, respectively, are listed.

t (a.u.)	$\Delta B^1_{21;20}$ (10^{-4} a.u.)	$\Delta B^1_{21;50}$ (10^{-4} a.u.)	$\Delta B^1_{21;20}$ (1–21) (10^{-4} a.u.)	$\Delta B^1_{21;20}$ (22–42) (10^{-4} a.u.)
0.5	−8.7	−38.9	1.5	−10.1
1.0	−24.8	−105.3	0.6	−25.3
1.5	−15.3	−44.3	−7.1	−8.2
2.5	31.8	126.4	−24.3	56.0
3.0	10.4	3.0	−20.0	30.4
5.0	6.8	45.8	6.2	0.6
8.0	−1.0	−8.0	−1.3	0.2

TABLE IV. Influence of compositional disorder on the autocorrelation function $B(t)$. The well parameter V has been modulated by $M\%$. For additional information see caption of Table III.

t (a.u.)	$\Delta B^1_{21;5}$ (10^{-4} a.u.)	$\Delta B^1_{21;8}$ (10^{-4} a.u.)	$\Delta B^1_{21;8}$ (1–21) (10^{-4} a.u.)	$\Delta B^1_{21;8}$ (22–42) (10^{-4} a.u.)
0.5	6.5	10.9	3.6	7.3
1.0	14.9	25.8	12.9	12.9
1.5	10.9	19.2	20.1	−0.9
2.5	−4.6	−7.5	1.6	−9.1
3.0	0.6	2.7	−14.3	17.0
5.0	−3.4	−6.1	−1.6	−4.5
8.0	−0.6	0.7	−4.1	4.7

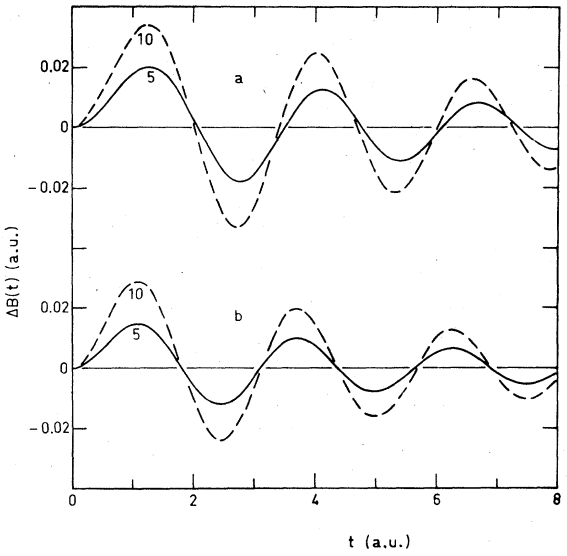

FIG. 11. Difference of autocorrelation functions of finite arrays with either vacancies (a) or interstitials (b) and the corresponding ordered arrays. The unit cell contains one well and the length of the array is 21 wells. Parameters for the ordered array are $a = 2$ a.u., $V = 3.6$ a.u., and $b = 0.5$ a.u. (a) One vacancy of width $w = 2$ a.u. at center of system (curve 5), two vacancies of width $w = 1.5$ a.u. symmetrically in the array (curve denoted by 10). (b) One interstitial with parameters $a_i = 2.4$ a.u. and $V_i = 3.2$ a.u. has replaced well 13 at center of system (curve denoted by 5), two interstitials with parameters $a_i = 2$ a.u., and $V_i = 3.2$ a.u. have replaced wells 6 and 13 symmetrically from center of system (curve denoted by 10). Number of bound states is in all cases 42 and norm $B(0) = 2$ a.u.

associated with the geometrical structure of the underlying system.

V. CONCLUSIONS

The results of our model study can be summarized as follows.

(i) The density of states, the one-electron density matrix, and the autocorrelation function converge with the system size such that a reasonable convergence is reached when the size of the system exceeds the maximum correlation length of interest by a factor of 2, as may be read off from Figs. 2, 3, 6, and 7 and Tables I and II. Consequently, these quantities are mainly determined by the microstructure within a relatively small part of the total system.

(ii) For molecules the number of zeros of $B(t)$ is related to the number of zeros of the atomic autocorrelation function and the number of atoms per molecule. Especially in the present one-dimensional case, we find the relation given in Eq. (6). The relation was also found to be valid for the unit cell of infinite ordered systems with filled bands. Similar relations exist also for real three-dimensional materials with completely filled bands.[5]

(iii) The zeros of the autocorrelation function of an ordered elemental insulator or semiconductor are related to characteristic separations, such as the atomic separations, of the system [see Eqs. (7)–(9)]. This has also been observed for real materials both experimentally and theoretically.[5] For ordered systems with partially filled bands (metallic systems), the zeros are related to the Fermi momentum (Fig. 5). An experimental verification has been given earlier.[22]

(iv) For metallic systems the oscillations of the autocorrelation function are on the average stronger than for the corresponding insulators, indicating an increase of the electron-electron correlation (Fig. 5).

(v) The autocorrelation function of a compound insulator or semiconductor performs an arithmetic average over both the atomic separations [Eqs. (7)–(9)] and the atomic potentials, as is evident from the comparison of Figs. 3 and 9.

(vi) The influence of pure structural or compositional disorder on the autocorrelation function of insulators is negligible (Tables III and IV). This results from a cancellation effect between the occupied states, clearly in contrast with the behavior of the density of states, which responds quite sensitively to both types of disorder (Fig. 8).

(vii) Defects and interstitials in moderate concentrations affect the autocorrelation function most at correlation lengths corresponding to the zeros of $B(t)$ (Fig. 11). These effects scale roughly with concentration. A low concentration of nearly free states introduces a slowly varying background to the autocorrelation function (Fig. 10).

The state of art in experimental Compton spectroscopy may be characterized by the following two numbers, namely, a typical overall momentum resolution (FWHM) of 0.3–0.5 a.u., and a statistical accuracy of the order of 1% at the center of the Compton line.[1] Via the convolution theorem the resolution function appears for the autocorrelation function as a multiplicative factor, which, e.g., for a Gaussian resolution function has a half width of 9.2–5.5 a.u., respectively, on the t axis. Since a statistical resolution of 10%, 1%, and 0.1% has a 50% effect on the autocorrelation function of an isolated well already at 4.5, 8.0, and 9.5 a.u., respectively, it must be concluded that at present reliable experimental data for $B(t)$ may be obtained at most up to values of t of the order of four times the width of the nearest-neighbor separation. The consequence of the above conclusions for the interpretation of the

experimental autocorrelation functions derived from inelastic scattering spectra of molecules and solids are then obvious.

First, it seems relatively easy to reproduce experimentally determined autocorrelation functions of large molecules and solids using the cluster approach, because of the good convergence properties with respect to the size of the cluster. This implies that the autocorrelation function may be used for testing various models for the microstructure of large molecules or solids. Second, the zeros of the autocorrelation function offer a relative straightforward procedure for the determination of the Fermi surface of metals[23] and of characteristic separations in semiconductors or insulators, the interpretation of which is not yet completely resolved. And, finally, it seems promising to use the autocorrelation function as a probe for localized defects such as vacancies, interstitials, donors, and acceptors, etc., in ordered or disordered host materials.[5] One might, for example, determine the concentration of these defects as well as the nature of the involved electronic states. First attempts along these lines have already been attempted for hydrogen in metals[9,10] and for hydrogenated amorphous silicon.[24] In the latter case the hydrogen concentration has been determined from the comparison of the Compton profiles of hydrogenated amorphous silicon and polycrystalline silicon, and reasonable agreement with previous estimates has been obtained.

ACKNOWLEDGMENTS

This work was initiated at the end of a two year visit of one of us (P.K.) to the Institute of Physics of the Universität Dortmund (Federal Republic of Germany). P.K. expresses his gratitude towards Prof. J. Treusch for the pleasant stay with his group. He also wants to thank the members of the experimental Compton group, Prof. U. Bonse, Dr. W. Schülke, and Dr. W. Schröder, for stimulating discussions. Further, he gratefully acknowledges the travel means provided by the Finnish Academy of Sciences, which was necessary for the completion of this work. Two of us (P.K. and H.I.) also would like to thank Prof. T. Stubb, head of the Electron Physics Laboratory, for stimulating interest and support. This work was in part supported by the Deutsche Forschungsgemeinschaft.

---

*Present address: Physikalisch Technische Bundesanstalt, D-3300 Braunschweig, Federal Republic of Germany.

[1]For a recent review, see *Compton Scattering*, edited by B. G. Williams (McGraw-Hill, New York, 1977).

[2]P. Eisenberger and W. C. Marra, Phys. Rev. Lett. 27, 1413 (1971); I. R. Epstein, J. Chem. Phys. 53, 4425 (1970); V. H. Smith, Jr., and M. H. Whangabo, Chem. Phys. 5, 234 (1974); W. A. Reed, P. Eisenberger, K. C. Pandey, and L. C. Snyder, Phys. Rev. B 10, 1507 (1974).

[3]U. Bonse, W. Schröder, and W. Schülke, Solid State Commun. 21, 807 (1977).

[4]P. Krusius, B. Kramer, O. Schütz, and J. Treusch, Solid State Commun. 21, 1127 (1977).

[5]B. Kramer, P. Krusius, W. Schröder, and W. Schülke, Phys. Rev. Lett. 38, 1227 (1977).

[6]P. M. Platzman and N. Tzoar, Phys. Rev. 139, A410 (1965).

[7]P. Eisenberger and P. M. Platzman, Phys. Rev. A 2, 415 (1970).

[8]K. Suzuki, F. Itoh, T. Honda, and M. Kuroha, Phys. Lett. A 57, 95 (1976).

[9]R. Lässer, Berichte der KFA-Jülich, Nr. 1492 (1978).

[10]P. Pattison, M. Cooper, R. Holt, J. R. Schneider, and N. Stump, Z. Phys. B 27, 205 (1977).

[11]B. Kramer, P. Krusius, W. Schröder, and W. Schülke, in *Proceedings of the Seventh International Conference on Amorphous and Liquid Semiconductors*, edited by W. E. Spear (University of Edinburgh, Edinburgh, 1977).

[12]F. Biggs, L. B. Mendelsohn, and J. B. Mann, At. Data Nucl. Data Tables 16, 201 (1975).

[13]P. Krusius, J. Phys. C 10, 1875 (1977).

[14]R. Heaton and E. Lafon, Phys. Rev. B 17, 1958 (1978).

[15]W. Schülke, Phys. Status Solidi B 62, 453 (1974).

[16]A. Seth and D. E. Ellis, J. Phys. C 10, 181 (1977).

[17]B. Kramer and P. Krusius, Phys. Rev. B 16, 5341 (1977).

[18]See, e.g., E. H. Lieb and D. Mattis, in *Mathematical Physics in One Dimension*, edited by E. H. Lieb and D. Mattis (Academic, New York, 1966).

[19]G. K. Kristiansen, BIT 3, 205 (1963).

[20]See, e.g, C. E. Fröberg, *Introduction to Numerical Analysis* (Addison-Wesley, Reading, 1972).

[21]The variance is defined by $\sigma^2=\sum_{i=1}^{M}(\Delta n_i)^2/M$ and the relative deviation by $\sigma/\sum_i n_i$. M is fixed by the minimum and maximum energies of the density of states and the resolution width chosen. For the lower and upper band groups one obtains for the relative deviation 0% and 0.16%, respectively, and for the total system 0.5%.

[22]P. Pattison and B. G. Williams, Solid State Commun. 20, 585 (1976).

[23]W. Schülke, Phys. Status Solidi B 80, K67 (1977).

[24]D. Wolf, Diploma thesis (University of Dortmund, Federal Republic of Germany, 1978) (unpublished).